AIAA JOURNAL
Vol. 30, No. 6, June 1992

Spatial Instability of a Swirling Jet—Theory and Experiment

C. Wu* and S. Farokhi†
University of Kansas, Lawrence, Kansas 66045
and
R. Taghavi‡
Sverdrup Technology, Inc., Brook Park, Ohio 44142

To develop a foundation for active shear-layer control with swirl, spatial instability of a rotating jet is investigated both experimentally and theoretically. The hydrodynamic stability analysis is applied to an inviscid incompressible top-hat jet, with a swirl distribution of solid-body rotation and free vortex in and outside the vortex core, respectively. Both plane and helical instability modes are examined; i.e., $m = 0, \pm 1, \pm 2, \pm 3$. It is found that the top-hat jet with Rankine vortex swirl distribution is unstable in all of the modes studied. The higher the positive helicity (i.e., many-lobed disturbances spinning in the same direction as the rotating jet), the less spatially unstable the jet behavior; the higher the negative helicity (i.e., many-lobed disturbances of opposite spin), the more spatially unstable this behavior becomes. A comparison is made between theoretical results and limited experimental data of a low-intensity swirling jet ($S = 0.12$) for plane wave excitation ($m = 0$). The trend of the initial growth of the instability waves in the near field is qualitatively captured by the inviscid linear instability theory when excitation amplitude is sufficiently small, e.g., less than 1% of the mean axial velocity. At higher forcing amplitudes, the nonlinear interactions will render the linear theory inadequate.

Nomenclature

A	= group parameter, $\alpha U - \omega + mW/r$
C_{p1}, C_{p2}	= constants in pressure equation
C_1, C_2, C_3	= constants in stability analysis
c	= disturbance phase speed
D, R	= nozzle exit diameter and radius, respectively
f	= excitation frequency
m	= azimuthal wave number
P	= instantaneous pressure
$\bar{P}$	= time-averaged pressure
r, θ, x	= radial, azimuthal, and axial coordinates, respectively
r_o	= matching radius of inner and outer tangential velocity distributions
S	= jet swirl number
St	= Strouhal number
t	= time
U, W	= time-averaged axial and tangential velocity components, respectively
U_o	= initial jet axial velocity (constant)
u, v, w	= axial, radial, and tangential velocity disturbances, respectively
u_f'	= rms amplitude of the fundamental wave axial velocity
α	= complex wave number, $\alpha_r + \alpha_i$
Γ	= constant circulation parameter
δ	= radial displacement of the free vortex sheet
ρ	= fluid density
Ω	= jet angular velocity
ω	= disturbance angular frequency, $2\pi f$

Subscripts

c	= centerline
ce	= centerline at nozzle exit
mean	= mass averaged
o	= exit quantity
∞	= ambient condition

Superscripts

$'$	= fluctuating components of velocity and pressure
$\hat{}$	= amplitude of velocity and pressure disturbances

Introduction

In recent years, mixing enhancement, suppression, and, in general, control of shear layers through artificial excitation have been amply demonstrated by many researchers. The single most important discovery that led to the outburst of research in this area was the discovery of large-scale coherent structures in the near field of mixing layers. The deterministic nature of these organized disturbance wave structures and their interactions prompted a search for resonating conditions between the applied external forcing and shear-layer growth rate or response. However, the nonlinear dynamics of the instability waves' interactions make the problem more complicated than its mass-spring-dashpot mechanical counterpart. These difficulties are experimentally overcome by a systematic search for the preferred forcing frequency, in the nondimensional Strouhal number form, and preferred excitation modes in free turbulent shear layers. A sound guiding light for experimental investigations of this nature is, however, found in theoretical hydrodynamic stability analysis of parallel shear flows. The present theoretical and experimental investigation of spatial instability characteristics of turbulent swirling jets is a major element of active control of rotating shear layers. The practical applications of this research will be found in new aircraft combustion chamber designs leading to higher combustion efficiencies through enhanced mixing, reduction of IR signature in stealth aircraft, advanced design of multistaged turbomachinery blading, and housing as well as vortex-lift devices for external aerodynamics.

Swirling jets exhibit distinctive characteristics that are absent in their nonrotating counterparts. For instance, swirling jets are primarily driven in the near field (i.e., $x/D < 5$) by the static pressure gradients in both axial and radial directions. Hence, the mechanism of jet spread in the near field of a

Received Feb. 27, 1991; presented as Paper 91-1771 at the AIAA 22nd Fluid Dynamics, Plasma Dynamics, and Lasers Conference, Honolulu, HI, June 24-26, 1991; revision received Sept. 17, 1991; accepted for publication Sept. 23, 1991.

*Graduate Research Assistant. Member AIAA.
†Associate Professor of Aerospace Engineering; Director of Flight Research Laboratory. Member AIAA.
‡Experimental Aerodynamic Engineer; currently Assistant Professor of Aerospace Engineering, University of Kansas, Lawrence, KS 66045. Member AIAA.

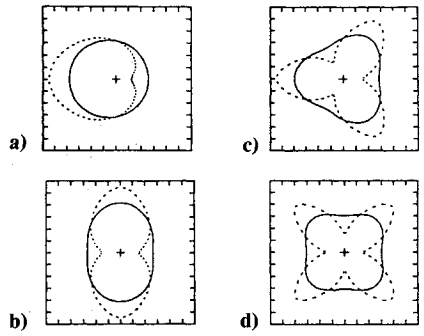

Fig. 1 Isovelocity contour plots with different helical mode excitation: a) $m = 1$; b) $m = 2$; c) $m = 3$; d) $m = 4$.[45]

swirling flow is mainly pressure driven. This is in contrast to nonrotating jets that are driven by turbulent mixing. An alternative view of the previously mentioned distinction is the absence of centrifugal instabilities in shear layers with zero rotation.

Farokhi et al.[1] have experimentally investigated the effect of initial swirl distribution, i.e., the manipulation of inertia terms, on the evolution of a turbulent jet. Their investigation clearly demonstrated the dominance of pressure gradient, induced by the vortex core, on the jet spread and vortex breakdown behavior.

A characteristic of swirling jets, namely, the presence of a centrifugal force, similar to buoyancy effect in stratified fluids, critically alters the stability characteristics of curved flows. The examples of Görtler instability leading to streamwise vortex structures in the boundary layer on a concave wall, Taylor vortices between two concentric cylinders with rotation, and the Crow instability of wingtip trailing vortices are classical examples that support the previous statement. Consequently, the instability characteristic of a swirling jet combines both Kelvin-Helmholz (shear) and Taylor-Görtler (centrifugal) instabilities.

Artificial excitation has been used by many researchers as an experimental tool for better understanding of laminar-to-turbulent transition and control of shear layers such as jets, wakes, and boundary layers. One of the principal applications of artificial excitation is in the study of flow instability. Axisymmetric jets without swirl are investigated thoroughly both theoretically and experimentally. The most important works have been done in the past few years, including Chan,[2] Crow and Champagne,[3] Michalke,[4] Hussain and Zaman,[5] Ahuja et al.,[6] and Cohen and Wygnanski[7]. It is demonstrated that nonswirling jets are excitable. Within the potential core, the axisymmetric disturbance is the dominant mode. Beyond the potential core, the first azimuthal mode is amplified. The first experimental investigation of controlled excitation of a turbulent swirling free jet was performed by Taghavi et al.[8] and Taghavi and Farokhi.[9] Their investigation confirmed the theoretical prediction of inviscid instability of a free swirling jet, based on the inflection point in the mean velocity profile in the shear layer, according to the classical hydrodynamic stability theory.[10] Although the experiment was limited to single-frequency plane-wave excitation, the fundamental rms amplitude of the disturbance wave was amplified in the near field (i.e., $x/D \leq 2.5$) at the preferred Strouhal number of 0.39. In comparison to the nonrotating jet, the fundamental instability wave in a swirling jet saturates closer to the jet exit and attains smaller amplitudes. Large-amplitude excitation of swirling turbulent jets, by Taghavi et al.,[11] resulted in the free jet mixing enhancement via plane acoustic waves. The rms growth of the fundamental disturbance along the jet centerline exhibited the classical hump and serves as a point of comparison with our theoretical investigation. The recent articles by Farokhi et al.,[12] Rice and Abbott,[13] and Rice and Zaman[14] highlight the current research in artificial excitation and its application to control of various turbulent shear layers.

In the classical hydrodynamic stability theory, the behavior of small wavy disturbances in parallel shear layers of prescribed mean velocity profile is studied. Earlier investigations were primarily based on temporal instability analysis of small perturbations in a parallel flow. However, as suggested by Watson,[15] Garg and Roleau,[16] and Michalke and Hermann,[17] spatial stability theory is more suitable for the study of near-field growth characteristics of the instability waves in shear flows. This is in fact consistent with the experimental results of Browand,[18] Mattingly and Chang,[19] Ho and Huang,[20] Gutmark and Ho,[21] and Thomas and Chu.[22] In addition, the theoretical results of Monkewitz and Huerre[23] and Huerre and Monkewitz[24] support the preceding assertion. For further comparisons between temporal and spatial instability theory, the reader is referred to Gaster[25] and Kelly.[26] The results of temporal stability analysis of various potential vortex and trailing line vortex flows are reported by Lessen et al.,[27,28] Khorrami et al.,[29] and Khorrami.[30] Spatial stability analysis of a slowly diverging jet, in the inviscid limit, is performed by Crighton and Gaster.[31] The instability modes of a diverging jet are found to be appreciably distorted, a fact of significant importance for the swirling jet instability analysis. The work of Ref. 31 is extended by Plaschko[32] to include helical instability modes in a slowly diverging jet. The results of spatial hydrodynamic stability analysis of inviscid incompressible, linearized small disturbances in a swirling jet are presented in this paper. The theoretical jet is assumed to have a top-hat axial velocity profile, solid-body rotation, and free vortex swirl distribution in and outside the vortex core, respectively. It has to be noted, however, that the preceding asumption of the mean velocity profile resembles the experimental jet only near the nozzle exit. Farther downstream, the assumption of top-hat mean axial velocity profile is no longer valid. Although the experimental data are limited to plane-wave excitation of a swirling free jet, the hydrodynamic stability analysis is performed for both plane and helical instability waves; i.e., $m = 0, \pm 1, \pm 2, \pm 3$, where $m = 0$ denotes the plane-wave excitation, $m = \pm 1$ identifies the first helical mode with one lobe, $m = \pm 2$ is the second helical wave with two lobes, and similarly for higher helical disturbances (see Fig. 1). Here, the positive and negative signs imply helical perturbation waves that spin in the same direction and opposite to the direction of the jet rotation, respectively.

Spatial Inviscid Instability Theory

The present theoretical study is limited to inviscid, linear hydrodynamic stability theory with local parallel flow assumption. The governing equations are the Euler and continuity equations in cylindrical coordinates, which in vector differential form are

$$\frac{\partial V}{\partial t} + V \cdot \nabla V = -\frac{1}{\rho}\nabla P \tag{1}$$

$$\nabla \cdot V = 0 \tag{2}$$

To perform linear hydrodynamic stability analysis, we assume that the instantaneous flowfield is composed of a time-averaged velocity and pressure field and traveling wave disturbances, namely,

$$V = \bar{V} + V' \tag{3}$$

$$P = \bar{P} + p' \tag{4}$$

where the perturbations in velocity and pressure take on the standard formulation:

$$V' = \{\hat{u}, i\hat{v}, \hat{w}\} \exp[i(\alpha x + m\theta - \omega t)] \tag{5}$$

$$p' = \hat{p} \exp[i(\alpha x + m\theta - \omega t)] \tag{6}$$

The linearizing assumptions in our analysis are $|V'|/V \ll 1$ and $p'/P \ll 1$.

In general, α is the axial wave number, m the azimuthal wave number, and ω the disturbance angular frequency. In the case of spatial instability analysis, α is set to be a complex quantity; i.e., $\alpha = \alpha_r + i\alpha_i$, where α_r is the real axial wave number and α_i is the spatial amplification rate. For positive α_i, the flow is stable, otherwise, the flow is unstable.

Upon substitution of Eqs. (3-6) into Eqs. (1) and (2) and invoking the linearization assumptions, we obtain the following four perturbation equations in terms of disturbance amplitudes $\hat{u}$, $\hat{v}$, $\hat{w}$, and $\hat{p}$:

$$A\hat{u} + \alpha\hat{p} = 0 \tag{7}$$

$$-A\hat{v} - \frac{2W}{r}\hat{w} + \frac{d\hat{p}}{dr} = 0 \tag{8}$$

$$\left(\frac{dW}{dr} + \frac{W}{r}\right)\hat{v} + A\hat{w} + \frac{m}{r}\hat{p} = 0 \tag{9}$$

$$\alpha\hat{u} + \frac{\hat{v}}{r} + \frac{d\hat{v}}{dr} + \frac{m}{r}\hat{w} = 0 \tag{10}$$

The disturbance boundary conditions are given at $r = 0$ by

$$\hat{v}(0) + \hat{w}(0) = 0, \qquad \hat{u}(0), \hat{p}(0)$$

must be finite for $m = 0$ (11a)

$$\hat{v}(0) + \hat{w}(0) = 0, \qquad \hat{u}(0) = \hat{p}(0) = 0 \qquad \text{for } m = \pm 1 \tag{11b}$$

$$\hat{u}(0) = \hat{v}(0) = \hat{w}(0) = \hat{p}(0) = 0 \qquad \text{for } |m| > 1 \tag{11c}$$

and at $r = \infty$ by

$$\hat{u}(\infty) = \hat{v}(\infty) = \hat{w}(\infty) = \hat{p}(\infty) = 0 \qquad \text{for all } m \tag{11d}$$

The perturbation equations (7-10) can be reduced to a linear second-order ordinary differential equation in $\hat{u}$:

$$\alpha^2\left[A^2 - 2\frac{W}{r}\left(\frac{dW}{dr} + \frac{W}{r}\right)\right]\frac{d}{dr}\left\{\frac{A\,d(A\hat{u})/dr + 2\dfrac{mAW}{r^2}\hat{u}}{\alpha^2\left[A^2 - 2\dfrac{W}{r}\left(\dfrac{dW}{dr} + \dfrac{W}{r}\right)\right]}\right\}$$

$$+\frac{A}{r}\frac{d(A\hat{u})}{dr} - \frac{m}{r}\left(\frac{dW}{dr} + \frac{W}{r}\right)\frac{d(A\hat{u})}{dr} + 2\frac{mAW}{r^3}\hat{u}$$

$$-\frac{m^2A^2}{r^2}\hat{u} - \alpha^2\left[A^2 - 2\frac{W}{r}\left(\frac{dW}{dr} + \frac{W}{r}\right)\right]\hat{u} = 0 \tag{12}$$

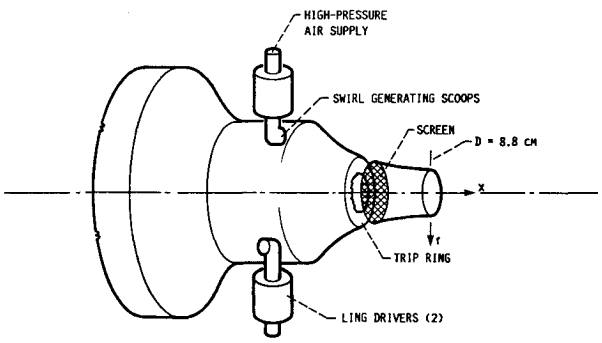

Fig. 2 Schematic drawing of jet facility.

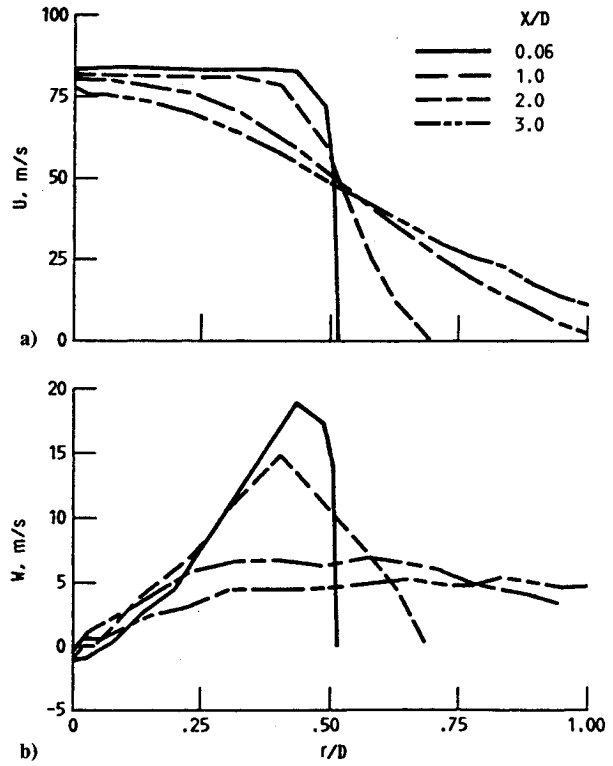

Fig. 3 Experimental measurements of downstream development of the time-mean velocity components—$S = 0.12$, $M = 0.22$: a) axial direction; b) tangential direction.

For the present investigation, the steady mean flowfield is assumed to be

$$U\begin{cases} = U_o, & 0 \le r \le r_o \\ = 0, & r_o \le r \le \infty \end{cases} \tag{13}$$

$$W\begin{cases} = \Omega r, & 0 \le r \le r_o \\ = \Gamma/r, & r_o \le r \le \infty \end{cases} \tag{14}$$

where r_o is the matching radius of solid-body rotation and potential vortex, Ω the angular velocity inside the matching radius, and Γ the constant circulation parameter outside the matching radius.

Within the solid-body rotation core, i.e., $0 \le r \le r_o$, Eq. 12 simplifies to a modified Bessel equation in $\hat{u}$:

$$\frac{d^2\hat{u}}{dr^2} + \frac{1}{r}\frac{d\hat{u}}{dr} - \left(\mu^2 + \frac{m^2}{r^2}\right)\hat{u} = 0 \tag{15}$$

With Eq. (15) and the specified boundary conditions, the perturbation equations (7-10) can be solved for the radial eigenfunctions as

$$\hat{u}(r) = C_1 I_m(\mu r) \tag{16a}$$

$$\hat{v}(r) = -iC_1\frac{\alpha}{\mu^2}\left\{\frac{2m\Omega}{(\alpha U_o + m\Omega - \omega)}I_m(\mu r) + \frac{dI_m(\mu r)}{dr}\right\} \tag{16b}$$

$$\hat{w}(r) = C_1\frac{\alpha}{\mu^2}\left\{\frac{m}{r}I_m(\mu r) + \frac{2\Omega}{(\alpha U_o + m\Omega - \omega)}\frac{dI_m(\mu r)}{dr}\right\} \tag{16c}$$

$$\hat{p}(r) = -C_1\frac{(\alpha U_o + m\Omega - \omega)}{\alpha}I_m(\mu r) \tag{16d}$$

where

$$\mu = \alpha\sqrt{1 - \frac{4\Omega^2}{(\alpha U_o + m\Omega - \omega)^2}} \tag{17}$$

where C_1 is a constant, and I_m is the modified Bessel function of the first kind.

In the outer potential vortex flow, i.e., $r_o \leq r \leq \infty$, Eq. (12) also simplifies to a modified Bessel equation in $\hat{u}$ as

$$\frac{d^2\hat{u}}{dr^2} + \frac{1}{r}\frac{d\hat{u}}{dr} - \left(\alpha^2 + \frac{m^2}{r^2}\right)\hat{u} = 0 \tag{18}$$

Now, with the far-field boundary conditions, Eqs. (18) and (7-10) can be solved for the radial eigenfunctions as

$$\hat{u}(r) = C_2 K_m(\alpha r) \tag{19a}$$

$$\hat{v}(r) = -iC_2\frac{1}{\alpha}\frac{dK_m(\alpha r)}{dr} \tag{19b}$$

$$\hat{w}(r) = C_2\frac{m}{\alpha r}K_m(\alpha r) \tag{19c}$$

$$\hat{p}(r) = C_2\frac{(\omega - m\Gamma/r^2)}{\alpha}K_m(\alpha r) \tag{19d}$$

where C_2 is a constant and K_m is the modified Bessel function of the second kind.

To constitute the eigenvalue problem, the free vortex sheet assumption is applied to the interface between the inner and outer flows. First we assume that, at the matching radius, the radial displacement of the vortex sheet due to disturbance is described by $\delta = C_3 \exp[i(\alpha x + m\theta - \omega t)]$, where C_3 is a constant. Applying the kinematic boundary condition at both sides of the matching radius, we get

$$\frac{D\delta}{Dt} = \frac{\partial\delta}{\partial t} + (V \cdot \nabla)\delta = v \tag{20}$$

In physical terms, the kinematic boundary condition on the wavy free vortex sheet described by Eq. (20) is the statement of flow tangency condition to the interface on both sides. Hence, both tangential and radial perturbations are discontinuous on the wavy interface, but their slopes are identical to the wave (see Refs. 33 and 34). The two radial perturbation velocities across the free vortex sheet can be obtained from Eq. (20).

Inner solution (i.e., $r \leq r_o$):

$$\frac{C_1\alpha}{\mu^2}\left\{\frac{2m\Omega}{Ar_o}I_m(\mu r_o) + \frac{dI_m(\mu r_o)}{dr}\right\} + C_3 A = 0 \tag{21}$$

Outer solution (i.e., $r \geq r_o$):

$$C_2\frac{dK_m(\alpha r_o)}{dr} + C_3\alpha\left(\frac{m\Gamma}{r^2} - \omega\right) = 0 \tag{22}$$

Finally, the dynamic boundary condition on a free vortex sheet demands the continuity of static pressure across the sheet as fluid material elements cannot sustain a static pressure jump. Hence, the dynamic boundary condition at the fluid interface requires

$$\bar{P}_1(r_o + \delta) + p_1 = \bar{P}_2(r_o + \delta) + p_2 \tag{23}$$

where

$$\frac{\bar{P}_1}{\rho} = \frac{1}{2}\Omega^2 r^2 + C_{p1}, \qquad \frac{\bar{P}_2}{\rho} = \frac{1}{2}\frac{\Gamma^2}{r^2} + C_{p2} \tag{24}$$

therefore,

$$C_1 A I_m(\mu r_o) - C_2\left(\frac{m\Gamma}{r^2} - \omega\right)K_m(\alpha r_o) + C_3\alpha\left(\frac{\Gamma^2}{r_0^3} - \Omega^2 r_o\right) = 0 \tag{25}$$

Eliminating the constants C_1, C_2, and C_3 from Eqs. (21), (22), and (25), we obtain the following eigenvalue problem:

$$\left\{\frac{2m\Omega^*}{(m\Omega^* + \alpha^* - \omega^*)}\frac{1}{r_o} + \frac{dI_m(\mu^*)/dr}{I_m(\mu^*)}\right\} \times \left\{(m\Gamma^* - \omega^*)^2\frac{K_m(\alpha^*)}{dK_m(\alpha^*)/dr}\right\} - [(m\Omega^* + \alpha^* - \omega^*)^2 - 4\Omega^{*2}] = 0 \tag{26}$$

where

$$\alpha^* = \alpha r_o, \quad \mu^* = \mu r_o, \quad \omega^* = \frac{\omega r_o}{U_o}, \quad \Gamma^* = \frac{\Gamma}{r_o U_o}, \quad \Omega^* = \frac{\Omega r_o}{U_o} \tag{27}$$

The eigenvalue problem of Eq. (26) has been solved numerically. A complex-valued Newton-Raphson method is applied to achieve convergence to an accurate eigenvalue from the guessed estimate. Given a set of parameters m, r_o, U_o, ω, Γ, and Ω, all the * parameters (e.g., ω^*, μ^*, Γ^*, and Ω^*) are calculated from Eqs. (27). Thus, the complex modified Bessel functions of the first and second kind, as well as their first derivatives, can be numerically evaluated. The convergence criterion is set at 10^{-5}. A properly guessed estimate of α is crucial to the solution technique employed in this study.

Experimental Facility

The experimental aspect of the present work was performed in the free-shear-layer facility at NASA Lewis Research Center.

Swirl Generator and Excitation Section

Figure 2 is a schematic of the free-shear-layer facility. Plane acoustic waves were generated by two Ling Model EPT-94B Electro-Pneumatic acoustic drivers, positioned 180 deg apart around a 15.4-in. (41-cm) cylindrical section and operated in phase. Each driver is an electrically controlled air modulator capable of generating 170 dB sound pressure level in the near field. The drivers were operated by an air supply of 124 psig (87,184 kg/m^2) at a maximum flow rate of 0.6 lb/s (0.27 kg/s). The air leaving the drivers was directed into the tangential direction by means of scoops. After leaving the plenum, the swirling air passed through a 30-mesh screen and a trip ring before entering the 3.5-in.-diam (8.89-cm-diam) nozzle. The motivations behind the screen were 1) reduction of jet turbulence, and 2) better mixed-out, solid-body-rotation profile in the swirl distribution. The reduction of swirl intensity by the screen was of no concern because low swirl number jets were the intended targets of our investigations. The trip-ring function was to insure the emergence of turbulent shear layer from the nozzle. The screen and trip ring were located 13 in. (33 cm) upstream of the nozzle exit where the diameter of the contracting section was 5.16 in. (13.1 cm). More detailed description of the facility can be found in Refs. 8, 9, 11, and 12.

Instrumentation

Three components of time-mean velocity, as well as static and total pressure, were measured by a five-hole pitot probe having a diameter of 0.125 in. (0.318 cm) at the measuring tip. The probe tip has a 45-deg cone angle, and the pressure ports are located at the midspan of the conical surface. The five-hole probe is self-nulling in the yaw direction, and the pitch angle, time-mean velocity components, as well as mean pressure are computed from the measured pressures and the probe calibration curves.

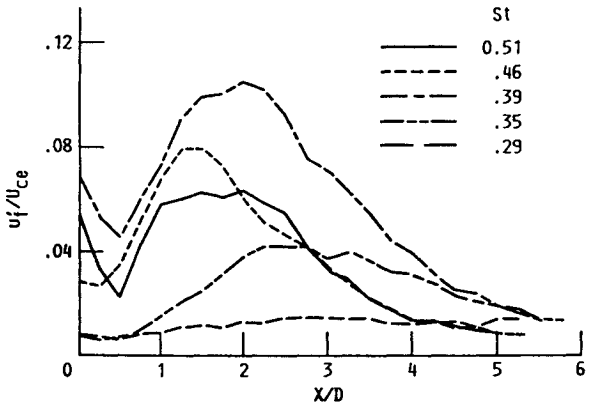

Fig. 4 Experimental measurements of growth of the fundamental wave along the jet centerline—$S = 0.12$, $M = 0.22$.

The axial component of fluctuating velocity was only measured along the jet centerline using a TSI mode 1260A-10 hot-wire probe and a DISA model 55M01 constant temperature employing a DISA model 55M25 linearizer. Along the jet axis, the tangential and radial velocity components are negligibly small compared to the axial component, and therefore, the results from a single-element hot-wire probe were assumed to represent the actual streamwise velocity fluctuations. The fundamental rms amplitude at each streamwise location was obtained by analyzing the hot-wire spectra at the excitation frequency. Although no phase-averaging technique was applied, the amplitude of the fundamental wave was significantly above the background noise, which insured negligible contamination of the instability-wave amplitude with background turbulent noise. To prevent the probe support from entering the flowfield and influencing the data due to its vibration, only half traverses were made starting from the jet centerline for the five-hole probe measurements.

Excitation pressure level and fluctuation pressure spectra, at the center of the nozzle exit, were measured using a model 4135 (B & K) microphone with a streamlined nose cone. The sound pressure level in decibels (re 20 μPa) at the excitation frequency was obtained from the spectra of the microphone signal using a Wavetek model 804A signal analyzer.

Test Conditions

The mass flow rate of 1.2 lb/s (0.54 kg/s) was designed for the experiment. The free jet was excited with a swirl number of $S = 0.12$ by plane acoustic waves. The maximum time-mean tangential and axial velocity at the nozzle exit plane were 58.8 fps (17.9 m/s) and 275 fps (83.8 m/s), respectively. The Mach and Reynolds numbers of the jet, based on the mass-averaged axial velocity at the nozzle exit and nozzle diameter, were 0.22 and 4.6×10^5, respectively. The maximum forcing amplitude of the plane-wave excitation was 6.88% of time-mean axial velocity at a Strouhal number of $St = 0.39$, measured at the center of the nozzle exit plane.

Experimental Results and Comparison with Linear Stability Theory

The free-shear-layer facility at NASA Lewis is utilized to investigate forced excitation of swirling jets. The first phase of shear-layer excitation research of rotating jets was limited to low swirl numbers. Here, the swirl number is defined, based on the time-averaged flow quantities, as

$$S = \frac{\int_0^\infty \rho U W r^2 \, dr}{R \int_0^\infty [\rho U^2 + (\bar{P} - P_\infty)] r \, dr} \tag{28}$$

which is essentially the ratio of jet mean torque to jet thrust nondimensionalized with the nozzle radius R. For the swirl number of $S = 0.12$, the mean axial velocity emerging from the nozzle describes a top-hat profile, as shown in Fig. 3a at $x/D = 0.066$. The initial mean swirl distribution is nearly solid-body rotation, as depicted in Fig. 3b at $x/D = 1.0$. Downstream development of the time-mean velocity components is shown in Fig. 3 for the jet mean swirl number $S = 0.12$ and the jet mass-averaged axial Mach number $M = 0.22$.

The jet was excited at various frequencies by plane acoustic waves; i.e., $m = 0$. The nondimensional parameter describing the forcing frequency is the Strouhal number defined as

$$St = \frac{fD}{U_{\text{mean}}} \tag{29}$$

The variation of the rms amplitude of the axial velocity fluctuations at the fundamental excitation frequency u_f', along the jet centerline, corresponding to various excitation Strouhal numbers, is shown in Fig. 4. The preferred Strouhal number was about 0.39, as indicated in the figure. The forcing amplitude of the excitation at this frequency was 6.88% of the time-mean centerline axial velocity at the nozzle exit (u_{fe}'/U_{ce}). The axial location of the saturation point was at $x/D = 2$. The trend of growth and decay of the instability wave agrees with the data of Mankbadi et al.[36] and Raman et al.[37] for highly turbulent nonswirling jets excited at high amplitudes. However, two major differences between the initial growth stages of the instability waves in swirling and nonrotating jets need to be pointed out. First, the location where maximum growth of the instability wave is reached for a swirling jet is much closer to the nozzle exit (namely, at $x/D = 2.0$ in our experiments) as compared to nearly 6 diameters for a nonrotating jet. Second, the amplitude of the instability wave in a swirling jet, at the location of maximum growth, is only a fraction (nearly one-half) of the corresponding nonrotating jet instability wave amplitude (see Ref. 11). These fundamental differences will be clarified by the spatial instability analysis in the present work.

Figure 5 shows, on a relative scale, the streamwise evolution of velocity spectra along the jet axis at an excitation frequency of 330 Hz ($St = 0.39$). The isolated peaks at 600 (first harmonic) and 990 Hz (second harmonic) can also be seen from Fig. 5 near the nozzle exit at $x/D = 0.06$. Since these higher harmonics were not amplified by the flow, their effects on the fundamental growth were not considered in this study. However, the excitation of these higher-frequency waves, i.e., $2f_e$ and $3f_e$, in our experimental setup leads to enhanced turbulence intensity near the jet exit, as shown by the analytical investigations of Mankbadi.[35] The mechanism behind such nonlinear wave-wave interactions in turbulent nonswirling jets is described by the integrated energy of the mean flow, coherent structures, and random turbulence in a cross section of the jet.[35] From Fig. 5, it is also evident that no growth of the subharmonic (165 Hz) is experienced in the case of the swirling jet excited by plane waves. This observation is in contrast to

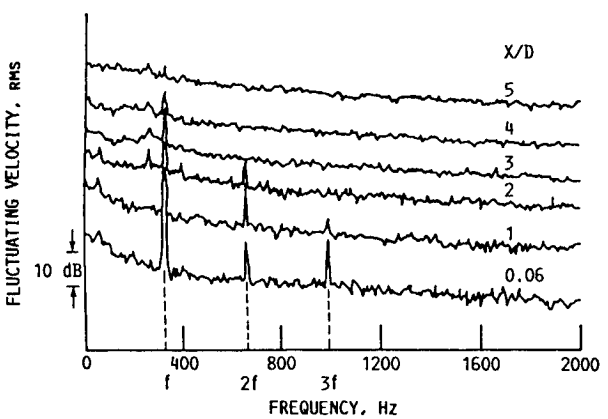

Fig. 5 Experimental measurements of evolution of u spectra along the jet axis—(relative scale) $St = 0.39$, $S = 0.12$, $M = 0.22$, bandwidth = 7.5 Hz.

those of the nonswirling jets, in which considerable growth of the subharmonic is measured as a result of excitation at the preferred Strouhal number of $St = 0.5$.[36,37]

Distributions of total axial turbulence intensity along the jet centerline for unexcited and excited ($St = 0.39$) cases are compared in Fig. 6a. It is seen that as a result of excitation the total turbulence intensity at the nozzle exit has been almost doubled and the location of its maximum value on the jet axis has moved upstream from $x/D = 6$ to 2.5. For a similar excited jet without swirl, the peak value is reached at a location much farther downstream ($x/D = 9$).[36] The swirling jet mixing enhancement due to forced excitation at preferred Strouhal number ($St = 0.39$) is indicated in Fig. 6b by faster decay of the mean centerline velocity than the unexcited jet. A 10% centerline mean axial velocity reduction is measured at $x/D = 9.0$.

The results of inviscid linear spatial instability analysis of the mean velocity profile described by a top-hat axial velocity, solid-body rotation, and free vortex swirl distributions in and outside the jet core, respectively, are shown in Fig. 7. Spatial amplification rate α_i of plane and six helical instability modes, as a function of real nondimensional frequency ω, is plotted for various circulation parameters. The top-hat jet with Rankine vortex-type swirl distribution is unstable to $m = 0$, 1, 2, 3, -1, -2, and -3 instability modes at all frequencies, as shown in Fig. 7. For a small circulation parameter $\Gamma = 0.1$, the plane and the four helical instability waves exhibit very similar amplification rates. Increasing the degree of rotation in the jet, or equivalently as Γ increases from 0.1 to 0.4, the negative helical instability modes show greater amplification rates than the plane and positive instability modes. The differences of amplification rates grow with increasing Γ. The third helical mode in the direction of shear-layer rotation (i.e., $m = 3$), though unstable, is the least amplified instability wave, whereas the third helical mode against the direction of shear-layer rotation (i.e., $m = -3$) is the most amplified instability wave, among the seven modes investigated in the near-field of the jet exit. Experimental investigations of Panda and Mclaughlin[38] and Panda[39] on the instabilities of swirling free jets, however, show nearly equal amplification rates of $m = -1$ and $+1$ helical instability modes; both helical modes

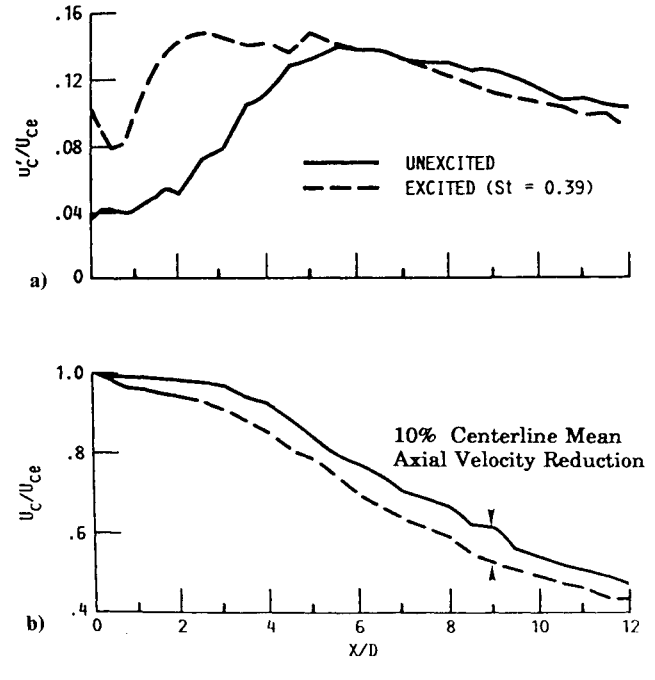

Fig. 6 Experimental measurements of effect of excitation of axial velocity components along the jet axis—$S = 0.12$, $M = 0.22$: a) rms fluctuations; and b) mean components.

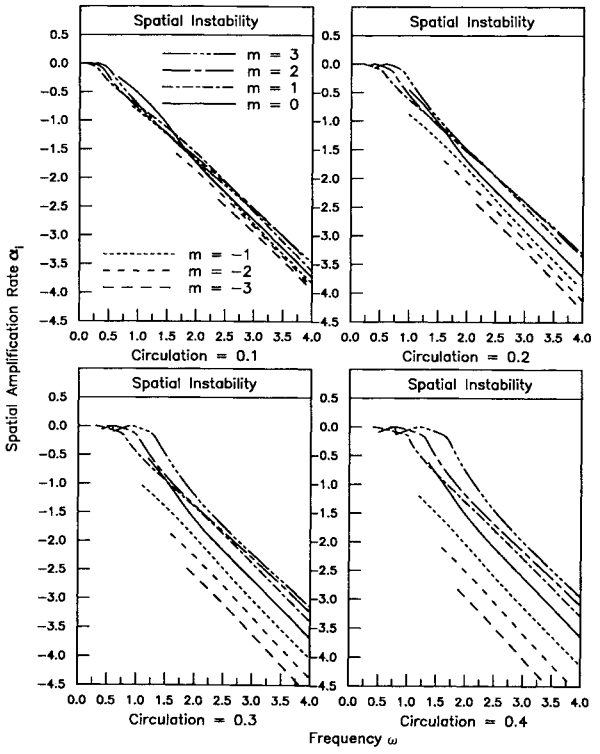

Fig. 7 Spatial amplification rate α_i for inviscid swirling jets, helical instability wave of $m = 0$, 1, 2, 3, -1, -2, -3 helicity, circulation parameter = 0.1, 0.2, 0.3, 0.4, respectively.

($m = \pm 1$) exhibited higher growth rates than the axisymmetric ($m = 0$) mode. The results of our analytical study, in general, agree with the latter and not with the former result of Panda.[39]

Inviscid modal instability of the theoretical swirling jet under consideration is shown in Fig. 8. The circulation parameter Γ is plotted as a running variable for $m = 2$, 0, -1, -3 instability modes. This depiction sheds light on the effect of rotation; i.e., centrifugal force on modal instability of swirling jets. For a corotating, two-lobed helical instability wave (i.e., $m = 2$), spatial amplification rate decreases with increasing degree of rotation. At higher excitation Strouhal numbers, however, the difference in amplification rates shrinks to a constant level. The axisymmetric mode ($m = 0$) exhibits nearly swirl independence in its spatial amplification rate behavior. As with all other modes investigated, the $m = 0$ mode experiences higher spatial growth rates with increasing excitation Strouhal number. Interestingly, the higher swirl enhances the growth of the helical instability waves of opposite spin; i.e., $m = -1$ and -3 (as shown in Fig. 8). This behavior is in contrast to the growth characteristics of positive helical modes and the degree of jet circulation. A plausible explanation of this changing behavior will be offered later. But first a major conclusion on the preferred mode of a swirling jet may be reached based on the results of our theoretical study. Namely, helical instability waves of negative spin (i.e., $m < 0$), preferably with more lobes in the azimuthal plane, which exhibit the highest spatial amplification rates, do constitute preferred modes of a swirling jet. Hence, artificial excitation of rotating shear layers with the intention of mixing enhancement must trigger helical instability waves of negative helicity for best results. This also explains, to some extent, Taghavi et al.'s result[8] that the plane-wave-excited swirling jet did not exhibit the same fundamental wave growth characteristics as a nonswirling jet excited by the axisymmetric mode. On the question of different amplification rates between the positive and negative helical instability waves in a swirling jet, one may seek an answer based on Taylor and Görtler centrifugal instabilities. First, we observe that a cospinning or counterspinning disturbance wave experiences the same Görtler instability because

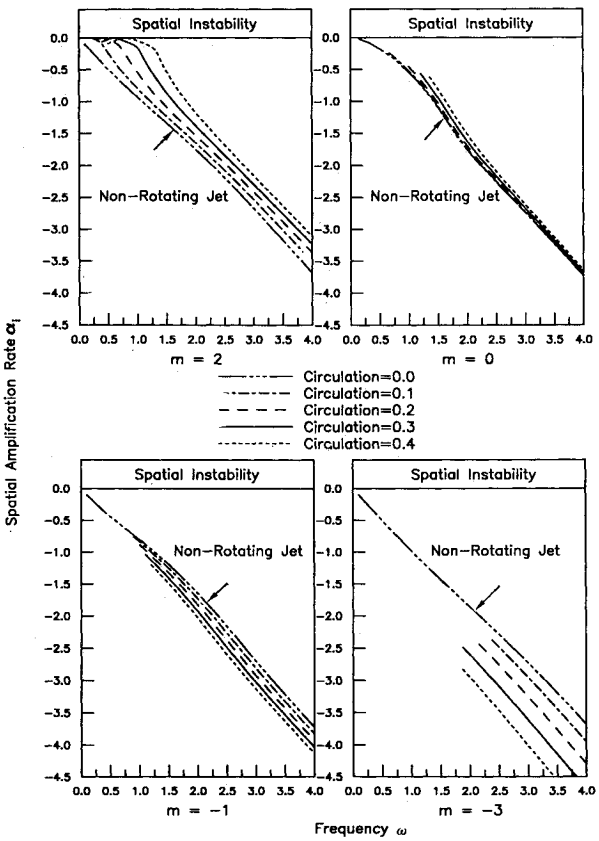

Fig. 8 Spatial amplification rate α_i for inviscid swirling jets, circulation parameter = 0.0, 0.1, 0.2, 0.3, 0.4, helical instability wave of $m = 2, 0, -1, -3$, respectively.

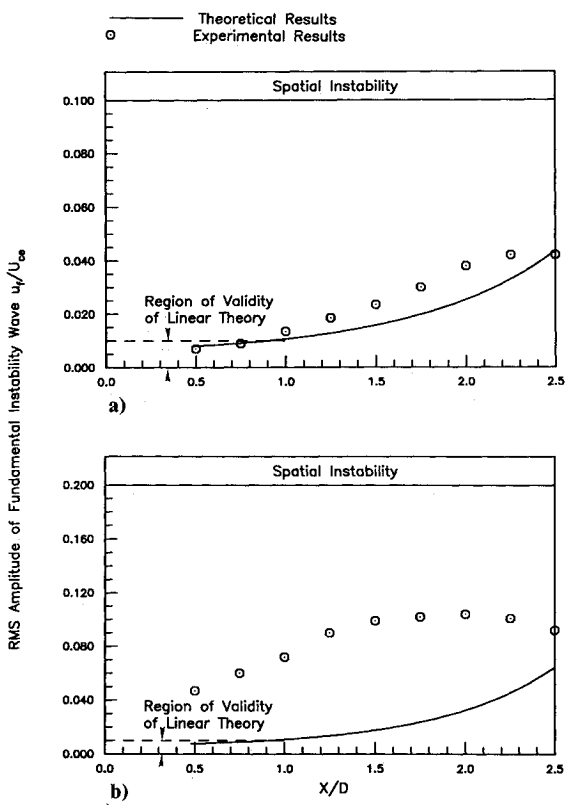

Fig. 9 Amplitude of fundamental wave along the jet axis for an inviscid swirling jet, plane instability wave ($m = 0$), swirl number $S = 0.12$, $M = 0.22$: a) $St = 0.35$; b) $St = 0.39$.

the spiral radius of curvature remains identical in the two cases. However, a counterspinning disturbance is more unstable in the sense of Taylor instability than a corotating one. Hence, enhanced Taylor instability offers a plausible answer to this question. Also, on the effect of jet circulation on the amplification rates of the helical instability waves, the preceding picture suggests that, as the Taylor instability wave grows with circulation, it feeds energy into counter-rotating disturbances while it absorbs energy from the cospinning waves. Future analytical investigations on nonlinear wave-wave interactions for swirling flows, similar to Mankbadi's[35] analysis of nonrotating jets, can shed light on the energy exchange mechanisms between the various components of swirling motion.

Experimental results of the rms amplitude of the fundamental wave, along the jet axis in the near field, is plotted in Fig. 9. The theoretical prediction of the hydrodynamic stability analysis based on the initial mean velocity profile is also shown in Fig. 9, with excitation Strouhal number $St = 0.35$ in Fig. 9a and $St = 0.39$ in Fig. 9b. It is to be noted in Fig. 9b that the forcing amplitude in the experiment generating 6.88% (see Fig. 4) of rms axial velocity fluctuation on the centerline at the nozzle exit is clearly beyond the scope of the linear theory. In fact, all forcing amplitudes greater than 1% are considered to fall in the nonlinear regime.[40] Consequently, the initial rms amplitude of the theoretical fundamental wave was only matched to the experimental one for the $St = 0.35$ case (see Fig. 9a). In Fig. 9a, a reasonable agreement between the theoretical results and the experimentally measured data is observed. The differences are primarily attributable to the following: 1) the assumed mean axial velocity profile of top hat not representing the measured mean axial velocity distribution in the jet beyond $x/D = 0.06$, 2) the linear theory not accounting for nonlinear wave-fine grain turbulence-mean flow interactions, and 3) parallel flow assumption. In the case of very large forcing amplitude, namely, the one depicted in Fig. 9b, we decided not to equate the initial theoretical rms amplitude of the fundamental disturbance wave based on linear theory to the experimentally generated disturbance well beyond the linear regime. The purpose of this portion of Fig. 9 is to demonstrate the inadequacy of the linear stability analysis in predicting the growth characteristic of nonlinear waves in turbulent shear layers.

Further analytical work to relax the top-hat limitation of the mean axial velocity profile is currently under way. The problem is further complicated by the lack of similarity profiles in the mean velocity distributions in the near field of swirling jets, as evidenced by detailed experimental work of Chigier and Chervinsky.[41,42] However, it has to be noted that a rotating jet attains similarity property farther downstream (i.e., $x/D \geq 4.0$, depending on swirling intensity) as closed-form solutions are obtained by Görtler[43] and Lee.[44]

Conclusions

An inviscid, spatial linear hydrodynamic stability analysis is performed on a jet with top-hat mean axial velocity, solid-body rotation, and potential vortex mean tangential velocity distributions in and outside of the jet, respectively. Seven instability modes, i.e., $m = \pm 3, \pm 2, \pm 1$, and 0 are investigated and found spatially unstable. Helical instability waves of negative spin are, however, the most amplified in the prescribed shear layer. Based on these theoretical results, helical disturbances that rotate in the opposite direction to the jet are identified as the preferred modes of a swirling jet. Spatial amplification rates of all instability waves monotonically grow with excitation frequency. Hence, no preferred Strouhal number is established by this theory in the range investigated. The effect of higher jet circulation enhances the spatial growth characteristics of $-m$ mode disturbances, whereas the opposite holds for $+m$ helical waves. Enhanced Taylor instability of disturbances with opposite spin offers a plausible rationale for this behavior. Interestingly, the spatial instability characteristic of the axisymmetric mode (i.e., $m = 0$) exhibits circula-

tion independence. Measurements along the axis of a plane-wave excited swirling jet showed the instability hump of the fundamental wave with, however, smaller saturation amplitude and closer-to-nozzle saturation location than the non-swirling jets. Reasonable agreement between the experimentally measured and theoretically predicted spatial instability wave growth is obtained in the near field when the rms excitation amplitude falls within the linear regime. Large-amplitude forcing of the instability waves is found to be beyond the scope of the linear analysis.

Acknowledgments

This work is supported by NASA Lewis Research Center under Grant NAG 3-1098. The authors would like to express their special appreciation to Edward J. Rice, K. Zaman, and R. Mankbadi of NASA Lewis Research Center for their valuable input and support of this work.

References

[1]Farokhi, S., Taghavi, R., and Rice, E. J., "Effect of Initial Swirl Distribution on the Evolution of a Turbulent Jet," *AIAA Journal*, Vol. 27, No. 6, 1989, pp. 700–706.

[2]Chan, Y. Y., "Spatial Waves in Turbulent Jets," *Physics of Fluids*, Vol. 17, No. 1, 1974, pp. 46–53.

[3]Crow, S. C., and Champagne, F. H., "Orderly Structure in Jet Turbulence," *Journal of Fluid Mechanics*, Vol. 48, Pt. 3, Aug. 1971, pp. 547–591.

[4]Michalke, A., "Survey on Jet Instability Theory," *Progress in Aerospace Sciences*, Vol. 21, No. 3, 1984, pp. 159–199.

[5]Hussain, A. K. M. F., and Zaman, K. M. B. Q., "The 'Preferred Mode' of the Axisymmetric Jet," *Journal of Fluid Mechanics*, Vol. 110, Sept. 1981, pp. 37–71.

[6]Ahuja, K. K., Lepicovsky, J., Tam, C. K. W., Morris, P. J., and Burrin, R. H., "Tone-Excited Jet—Theory and Experiment," NASA CR-3538, Nov. 1982.

[7]Cohen, J., and Wygnanski, I., "The Evolution of Instabilities in the Axisymmetric Jet. Part I," *Journal of Fluid Mechanics*, Vol. 176, March 1987, pp. 191–235.

[8]Taghavi, R., Rice, E. J., and Farokhi, S., "Large Amplitude Acoustic Excitation of Swirling Turbulent Jets," AIAA Paper 89-0970, March 1989.

[9]Taghavi, R., and Farokhi, S., "Turbulent Swirling Jets with Excitation," NASA CR-180895, March 1988.

[10]Lin, C. C., *The Theory of Hydrodynamic Stability*, Cambridge University Press, London 1955.

[11]Taghavi, R., Rice, E. J., and Farokhi, S., "Controlled Excitation of a Cold Turbulent Swirling Free Jet," *Journal of Vibration, Acoustics, Stress, and Reliability in Design*, Vol. 110, No. 2, 1988, pp. 234–237.

[12]Farokhi, S., Taghavi, R., and Rice, E. J., "Modern Developments in Shear Flow Control with Swirl," *Proceedings of the 17th Congress of the International Council of Aeronautical Sciences*, AIAA, Washington, DC, 1990; also, NASA CR-186586, May 1990.

[13]Rice, E. J., and Abbott, J. M., "Control of Flow Separation & Mixing by Aerodynamic Excitation," *Proceedings of the 17th Congress of the International Council of Aeronautical Sciences*, AIAA, Washington, DC, 1990.

[14]Rice, E. J., and Zaman, K. B. M. Q., "Control of Shear Flow by Artificial Excitation," NASA TM-100201; also, AIAA Paper 87-2722, Oct. 1987.

[15]Watson, J., "On Spatially-growing Finite Disturbances in Plane Poiseuille Flow," *Journal of Fluid Mechanics*, Vol. 14, Oct. 1962, pp. 211–221.

[16]Garg, V. K., and Roleau, W. T., "Linear Spatial Stability of Pipe Poiseuille Flow," *Journal of Fluid Mechanics*, Vol. 54, Pt. 1, July 1972, pp. 113–127.

[17]Michalke, A., and Hermann, G., "On the Inviscid Instability of a Circular Jet with External Flow," *Journal of Fluid Mechanics*, Vol. 114, Jan. 1982, pp. 3443–359.

[18]Browand, F. K., "An Experimental Investigation of the Instability of an Incompressible, Separated Shear Layer," *Journal of Fluid Mechanics*, Vol. 26, Oct. 1966, pp. 281–307.

[19]Mattingly, G. E., and Chang, C. C., "Unstable Waves on an Axisymmetric Jet Column," *Journal of Fluid Mechanics*, Vol. 65, Sept. 1974, pp. 541–560.

[20]Ho, C. M., and Huang, L. S., "Subharmonics and Vortex Merging in Mixing Layers," *Journal of Fluid Mechanics*, Vol. 119, June 1982, pp. 443–473.

[21]Gutmark, E., and Ho, C. M., "Preferred Modes and Spreading Rates of Jets," *Physics of Fluids*, Vol. 26, No. 10, 1983, pp. 2932–2938.

[22]Thomas, F. O., and Chu, H. C., "An Experimental Investigation of the Transition of a Planar Jet: Subharmonic Suppression and Upstream Feedback," *Physics of Fluids A*, Vol. 1, No. 9, 1989, pp. 1566–1587.

[23]Monkewitz, P. A., and Huerre, P., "Influence of the Velocity Rates on the Spatial Instability of Mixing Layers," *Physics of Fluids*, Vol. 25, July 1982, pp. 1137–1143.

[24]Huerre, P., and Monkewitz, P. A., "Absolute and Convective Instabilities in Free Shear Layers," *Journal of Fluid Mechanics*, Vol. 159, Oct. 1985, pp. 151–168.

[25]Gaster, M., "A Note on the Relation between Temporally-increasing and Spatially-increasing Disturbances in Hydrodynamic Stability," *Journal of Fluid Mechanics*, Vol. 14, Oct. 1962, pp. 222–224.

[26]Kelly, R. E., "On the Stability of an Inviscid Shear Layer which is Periodic in Space and Time," *Journal of Fluid Mechanics*, Vol. 27, March 1967, pp. 657–689.

[27]Lessen, M., Deshpande, N. V., and Hadji-Ohanes, B., "Stability of a Potential Vortex with a Non-rotating and Rigid-body Rotating Top-hat Jet Core," *Journal of Fluid Mechanics*, Vol. 60, Pt. 3, Sept. 1973, 459–4366.

[28]Lessen, M., Singh, P. J., and Paillet, F., "The Stability of a Trailing Line Vortex, Part 1: Inviscid Theory," *Journal of Fluid Mechanics*, Vol. 63, Pt. 4, May 1974, pp. 753–764.

[29]Khorrami, M. R., Malik, M. R., and Ash, R. L., "Application of Spectral Collocation Techniques to the Stability of Swirling Flows," *Journal of Computational Physics*, Vol. 81, No. 1, 1989, pp. 206–229.

[30]Khorrami, M. R., "On the Viscous Modes of Instability of a Trailing Line Vortex," *Journal of Fluid Mechanics*, Vol. 225, April 1991, pp. 197–212.

[31]Crighton, D. G., and Gaster, M., "Stability of Slowly Diverging Jet Flow," *Journal of Fluid Mechanics*, Vol. 77, Pt. 2, Sept. 1976, pp. 397–413.

[32]Plaschko, P., "Helical Instabilities of Slowly Diverging Jets," *Journal of Fluid Mechanics*, Vol. 92, Pt. 2, May 1979, pp. 209–215.

[33]Miles, J. W., "On the Reflection of Sound at an Interface of Relative Motion," *Journal of the Acoustical Society of America*, Vol. 29, No. 2, 1957, pp. 226–228.

[34]Ribner, H. S., "Reflection, Transmission, and Amplification of Sound by a Moving Medium," *Journal of the Acoustical Society of America*, Vol. 29, No. 4, 1957, pp. 435–441.

[35]Mankbadi, R. R., "Multifrequency Excited Jets," *Physics of Fluid A*, Vol. 3, No. 4, 1991, pp. 595–605.

[36]Mankbadi, R., Raman, G., and Rice, E. J., "Effects of Core Turbulence on Jet Excitability," AIAA Paper 89-0966, March 1989.

[37]Raman, G., Zaman, K. M. B. Q., and Rice, E. J., "Initial Turbulence Effect on Jet Evolution With and Without Tonal Excitation," AIAA Paper 87-2725, Oct. 1987; also, NASA TM-100178, Oct. 1987.

[38]Panda, J., and Mclaughlin, D. K., "Instabilities in a Free Swirling Jet," AIAA Paper 90-0506, Jan. 1990.

[39]Panda, J., "Experiments on the Instabilities in Swirling and Non-swirling Free Jets," Ph.D. Dissertation, Aerospace Engineering Dept., Pennsylvania State Univ., University Park, PA, Dec. 1990.

[40]Rice, E. J., Zaman, K. M. B. Q., and Raman, G., private communication, Aug. 1990.

[41]Chigier, N. A., and Chervinsky, A., "Experimental and Theoretical Study of Turbulent Swirling Jets Issuing from a Round Orifice," *Israel Journal of Technology*, Vol. 4, No. 1-2, 1966, pp. 44–54.

[42]Chigier, N. A., and Chervinsky, A., "Experimental Investigation of Swirling Vorted Motion in Jets," *Journal of Applied Mechanics*, Vol. 34, June 1967, pp. 443–451.

[43]Görtler, H., "Decay of Swirl in an Axially Symmetrical Jet, Far from the Orifice," *Reviista, Matemática Hispanoaméricas*, Vol. 14, Series 4, Nos. 4, 5, 1954, pp. 143–178.

[44]Lee, S. L., "Axisymmetrical Turbulent Swirling Jet," *Journal of Applied Mechanics*, Vol. 32, June 1965, pp. 258–262.

[45]Cohen, J., and Wygnanski, I., "The Evolution of Instabilities in the Axisymmetric Jet. Part 2. The Flow Resulting from the Interaction Between Two Waves," *Journal of Fluid Mechanics*, Vol. 176, March 1987, pp. 221–235.